

Signatures of the strongly interacting QGP in relativistic heavy-ion collisions

E.L. Bratkovskaya^a, O. Linnyk^a, V.P. Konchakovski^b,
M.I. Gorenstein^c, W. Cassing^b

^a*Institut für Theoretische Physik, Goethe-Universität Frankfurt am Main, Germany*

^b*Institut für Theoretische Physik, Justus-Liebig-Universität Giessen, Germany*

^c*Bogolyubov Institute for Theoretical Physics, Ukraine*

Abstract

The transition from hadronic to partonic degrees of freedom in the course of a relativistic heavy-ion collision is described by the microscopic covariant Parton-Hadron-String Dynamics (PHSD) transport approach. Studying Pb+Pb reactions from 40 to 158 A·GeV and comparing the PHSD results to those of the Hadron-String Dynamics (HSD) approach without a phase transition to the QGP, we observe that the existence of the partonic phase has a sizable influence on the transverse mass distribution of final kaons due to the repulsive partonic mean fields. Furthermore, we find a significant effect of the QGP on the production of multi-strange antibaryons due to a slightly enhanced $s\bar{s}$ pair production in the partonic phase from massive time-like gluon decay and to a more abundant formation of strange antibaryons in the hadronization process. Another evidence for pre-hadronization dynamics is gained from a study of di-jet correlations in Au+Au collisions at the top RHIC energy of $\sqrt{s} = 200$ GeV. Within the HSD transport approach, the reaction of the hadronic medium to the jet energy loss is calculated. In comparison with the data of the STAR, PHOBOS and PHENIX Collaborations differentially in azimuthal angle and pseudorapidity, the HSD results do not show enough suppression for the ‘away-side’ jet. In addition, the HSD results exhibit neither a ‘Mach-cone’ structure for the angular distribution in the away-side jet nor the ‘ridge’ long-range rapidity correlations for the near-side jet as observed by the STAR and PHOBOS Collaborations, thus suggesting a partonic origin of these structures.

The nature of confinement and the phase transition from a partonic system of quarks, antiquarks and gluons – a quark-gluon plasma (QGP) – to interacting hadrons, as occurring in relativistic nucleus-nucleus collisions, is a central topic of modern high-energy physics. In the present work, the dynamical evolution of the heavy ion-collision is described by the PHSD transport approach [1] incorporating the off-shell propagation of the partonic quasi-particles according to [2] as well as the transition

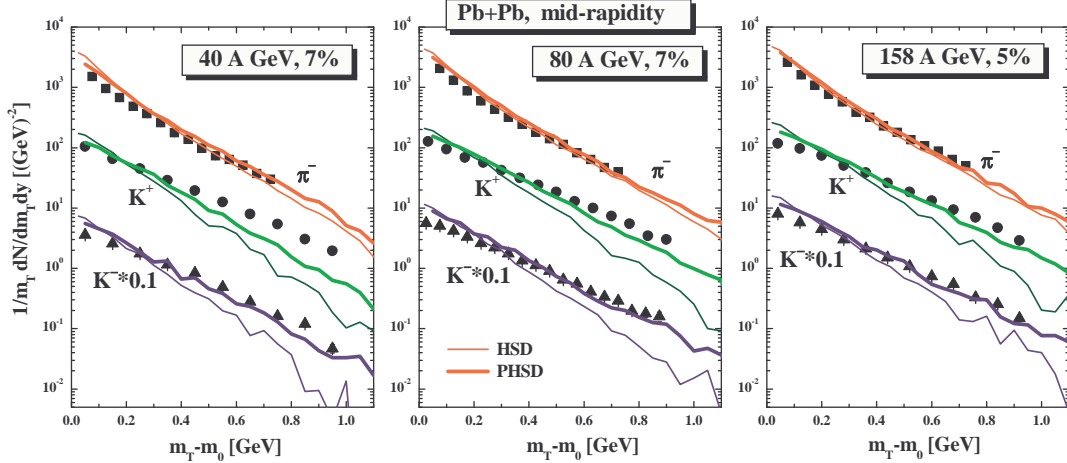


Fig. 1. The π^- , K^+ and K^- transverse mass spectra for central Pb+Pb collisions at 40, 80 and 158 A·GeV from PHSD (thick solid lines) in comparison to the distributions from HSD (thin solid lines) and the experimental data from the NA49 Collaboration [13].

to resonant hadronic states (or strings). In Section 2, we employ the PHSD approach – described in Section 1 and in more detail in [1,3] – to strangeness production in nucleus-nucleus collisions at moderate relativistic energies, i.e. at SPS energies up to 160 A·GeV. On the other hand, one should look within the same approach at the whole spectrum of observables with a special sensitivity to the partonic phase, e.g. strangeness [3], dileptons [4], charm [5], jets [6], etc. In this spirit, we dedicate Section 3 to a discussion of the medium reaction to the jet energy loss in Au+Au collisions at the top RHIC energy of $\sqrt{s} = 200$ GeV.

1 The PHSD approach

A consistent dynamical approach – valid also for strongly interacting systems – can be formulated on the basis of the Kadanoff-Baym equations [7,8] or off-shell transport equations in phase-space representation, respectively [2,8]. In the Kadanoff-Baym theory the field quanta are described in terms of propagators with complex selfenergies. Whereas the real part of the selfenergies can be related to mean-field potentials, the imaginary parts provide information about the lifetime and/or reaction rates of time-like ‘particles’ [9]. Once the proper (complex) selfenergies of the degrees of freedom are known, the time evolution of the system is fully governed by off-shell transport equations (as described in Refs. [2,8]).

The PHSD approach is a microscopic covariant transport model that incorporates effective partonic as well as hadronic degrees of freedom and involves a dynamical description of the hadronization process from partonic to hadronic matter [1]. Whereas the hadronic part is essentially equivalent to the conventional HSD approach [10] the partonic dynamics is based on the Dynamical QuasiParticle Model (DQPM) [11] which describes QCD properties in terms of single-particle Green’s functions (in the sense of a two-particle irreducible approach) and leads to effective strongly interacting partonic quasiparticles with broad spectral functions as degrees of freedom.

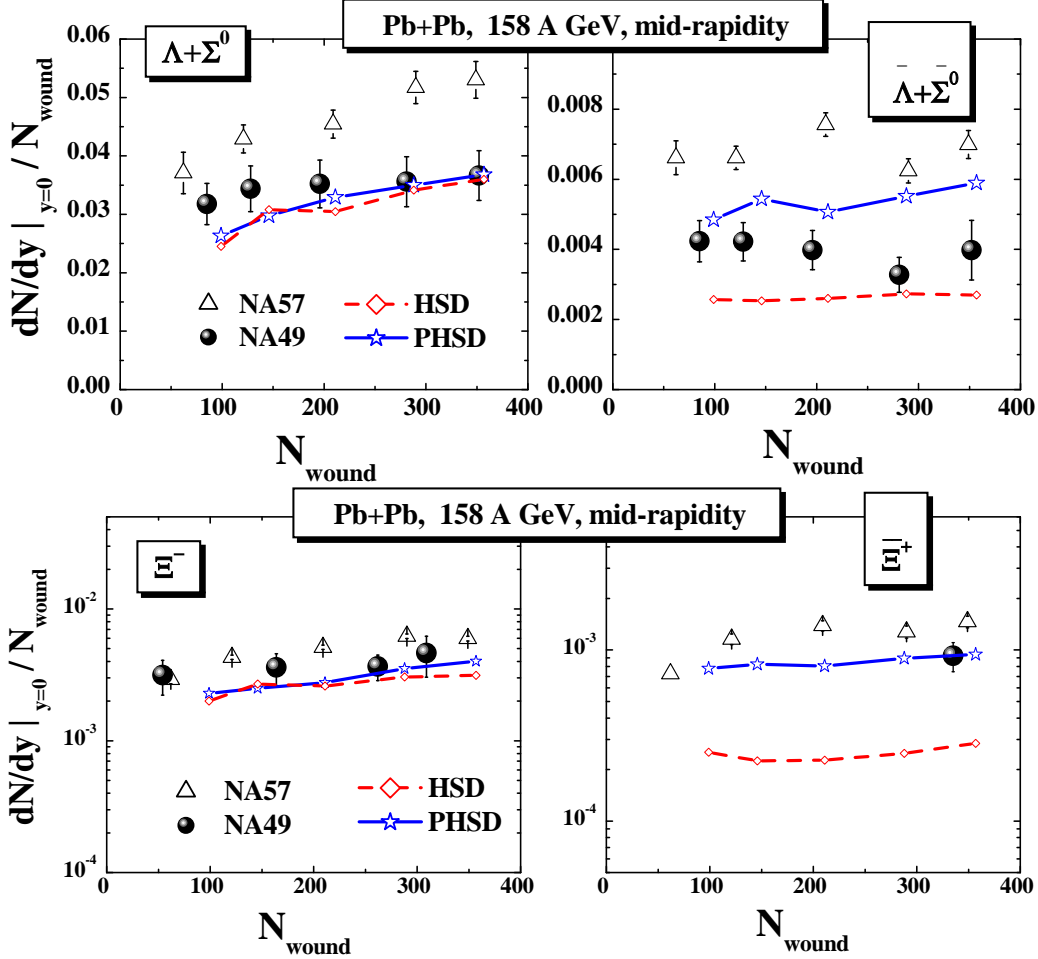


Fig. 2. **Top:** The multiplicities of $(\Lambda + \Sigma^0)/N_{wound}$ (l.h.s.) and $(\bar{\Lambda} + \bar{\Sigma}^0)/N_{wound}$ (r.h.s.) as a function of the number of wounded nucleons for Pb+Pb collisions at 158 A·GeV at mid-rapidity from PHSD (blue solid lines) and HSD (red dashed-dotted lines) in comparison to the experimental data from the NA57 Collaboration [15] (open triangles) and the NA49 Collaboration [16] (solid dots). The calculations have an error of 5–10% due to limited statistics. **Bottom:** The multiplicities of Ξ^-/N_{wound} (l.h.s.) and $\bar{\Xi}^+/N_{wound}$ (r.h.s.) vs N_{wound} for Pb+Pb collisions at 158 A·GeV at mid-rapidity. Line coding as above.

The off-shell parton dynamics also allows for a solution of the hadronization problem: the hadronization occurs by quark-antiquark fusion or 3 quark/3 antiquark recombination which is described by covariant transition rates as introduced in Refs. [3,1], obeying flavor current-conservation, color neutrality as well as energy-momentum conservation. Since the dynamical quarks become very massive close to T_c , the formed resonant 'pre-hadronic' color-dipole states ($q\bar{q}$ or qqq) are of high invariant mass, too, and sequentially decay to the ground-state meson and baryon octets increasing the total entropy. This solves the entropy problem in hadronization in a natural way [12].

2 Particle spectra in comparison to experiment

It is of interest, how the PHSD approach compares to the HSD [10] model (without explicit partonic degrees-of-freedom) as well as to experimental data. In Fig. 1 we

show the transverse mass spectra of π^- , K^+ and K^- mesons for 7% central Pb+Pb collisions at 40 and 80 A·GeV and 5% central collisions at 158 A·GeV in comparison to the data of the NA49 Collaboration [13]. Here the slope of the π^- spectra is only slightly enhanced in PHSD relative to HSD which demonstrates that the pion transverse motion shows no sizeable sensitivity to the partonic phase. However, the K^\pm transverse mass spectra are substantially hardened with respect to the HSD calculations at all bombarding energies - i.e. PHSD is more in line with the data - and thus suggest that partonic effects are better visible in the strangeness-degrees of freedom. The hardening of the kaon spectra can be traced back to parton-parton scattering as well as a larger collective acceleration of the partons in the transverse direction due to the presence of repulsive vector fields for the partons. The enhancement of the spectral slope for kaons and antikaons in PHSD due to collective partonic flow shows up much clearer for the kaons due to their significantly larger mass (relative to pions). We recall that in Refs. [22] the underestimation of the K^\pm slope by HSD (and also UrQMD) had been suggested to be a signature for missing partonic degrees of freedom; the present PHSD calculations support this early suggestion.

The strange antibaryon sector is of further interest since here the HSD calculations have always underestimated the yield [14]. In this respect we compare in Fig. 2 (top part) the multiplicities of $(\Lambda + \Sigma^0)/N_{wound}$ (l.h.s.) and $(\bar{\Lambda} + \bar{\Sigma}^0)/N_{wound}$ (r.h.s.) as functions of the number of wounded nucleons N_{wound} for Pb+Pb collisions at 158 A·GeV at mid-rapidity from PHSD and HSD to the experimental data from the NA57 Collaboration [15] and the NA49 Collaboration [16]. Whereas the HSD and PHSD calculations both give a reasonable description of the $\Lambda + \Sigma^0$ yield of the NA49 Collaboration, both models underestimate the NA57 data (open triangles) by about 30%. An even larger discrepancy in the data from the NA49 and NA57 Collaborations is seen for $(\bar{\Lambda} + \bar{\Sigma}^0)/N_{wound}$ (r.h.s.); here the PHSD calculations give results which are in between the NA49 data (solid dots) and the NA57 data (open triangles). We see that HSD underestimates the $(\bar{\Lambda} + \bar{\Sigma}^0)$ midrapidity yield at all centralities. This observation points towards a partonic origin but needs further examination.

The latter result suggests that the partonic phase does not show up explicitly in an enhanced production of strangeness (or in particular strange mesons and baryons) but leads to a different redistribution of antistrange quarks between mesons and antibaryons. To examine this issue in more detail we show in Fig. 2 (bottom part) the multiplicities of Ξ^- baryons (l.h.s.) and $\bar{\Xi}^+$ antibaryons (r.h.s.) - divided by N_{wound} - as a function of the number of wounded nucleons for Pb+Pb collisions at 158 A·GeV at mid-rapidity from PHSD and HSD in comparison to the experimental data from the NA57 Collaboration [15] and the NA49 Collaboration [17,16]. The situation is very similar to the case of the strange baryons and antibaryons before: we find no sizeable differences in the double strange baryons from HSD and PHSD - in a good agreement with the NA49 data - but observe a large enhancement in the double strange antibaryons for PHSD relative to HSD.

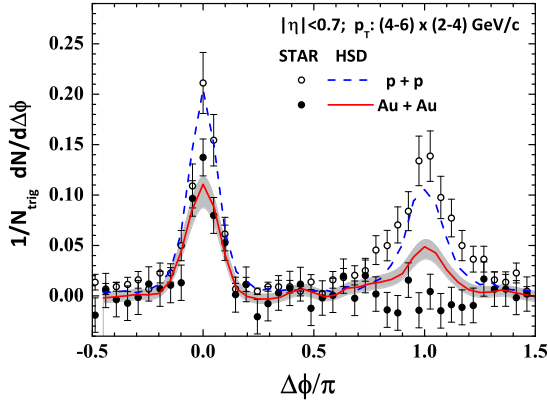


Fig. 3. Angular correlations of associated particles ($2 < p_T^{assoc} < 4$ GeV/c) with respect to a trigger particle with $p_T^{trig} > 4$ GeV/c in p+p and in central Au+Au collision events within the HSD transport approach in comparison to the STAR data [18]. The grey area corresponds to the statistical uncertainties of the HSD calculations.

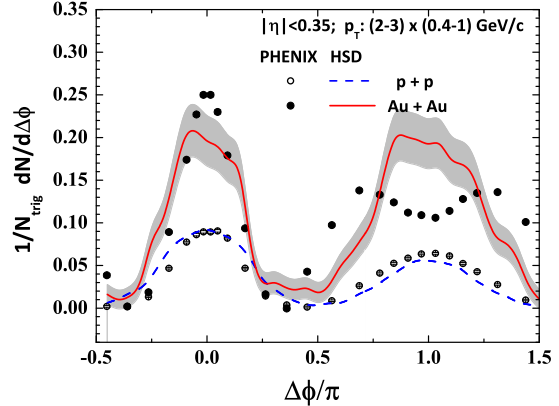


Fig. 4. Angular correlations of associated particles in p+p and in central Au+Au collisions within the HSD transport approach in comparison to the PHENIX data [19] at trigger transverse momentum $p_T^{trig} = 2 \div 3$ GeV/c and the associated particle transverse momentum $p_T^{assoc} = 0.4 \div 1$ GeV/c. The grey areas correspond to the statistical uncertainties of the HSD calculations.

3 Di-jet correlations at RHIC energies

Di-hadron correlations measure the associated particle distribution in azimuthal angle $\Delta\phi$ and pseudorapidity $\Delta\eta$ with respect to the high- p_T ‘trigger’ particle. The data on two-particle spectra in the high- p_T region in Au+Au collisions for the c.m.s. energy of the nucleon pair $\sqrt{s_{NN}} = 200$ GeV can be summarized as follows: 1) a strong suppression of the away-side hadrons (jet quenching) [18,19]; 2) a specific ‘Mach-cone’ structure in azimuthal angle $\Delta\phi$ in the region of the away-side jet [19]; 3) a long-range in pseudorapidity $\Delta\eta$ correlation (‘ridge’) in the region of the near-side jet [20,21]. The long-range correlations in $\Delta\eta$ might be a consequence of string-like correlation phenomena. In order to explore especially the conjecture of string-like correlations, we use the HSD model for the study of di-jet correlations, which employs dominantly early string formation in elementary reactions and their subsequent decay as well as hadronic and prehadronic interactions.

The previous HSD analysis of high- p_T spectra in Refs. [6,23] includes all model details and discusses the nuclear modification factor $R_{AA}(p_T)$ as the function of p_T and centrality. In extension of the previous investigations we now include the full evolution of jets in the transport approach including the response of the medium, which is important as the ‘Mach-cone’ and ‘ridge’ structures are attributed to medium evolution effects due to jet-medium interactions. In the current HSD calculations we use approximately 30×10^6 of p+p inelastic collision events and 0.5×10^6 of central Au+Au collisions with impact parameter $b = 0$. We use the mixed events method which allows to properly subtract the background by taking associated particles for

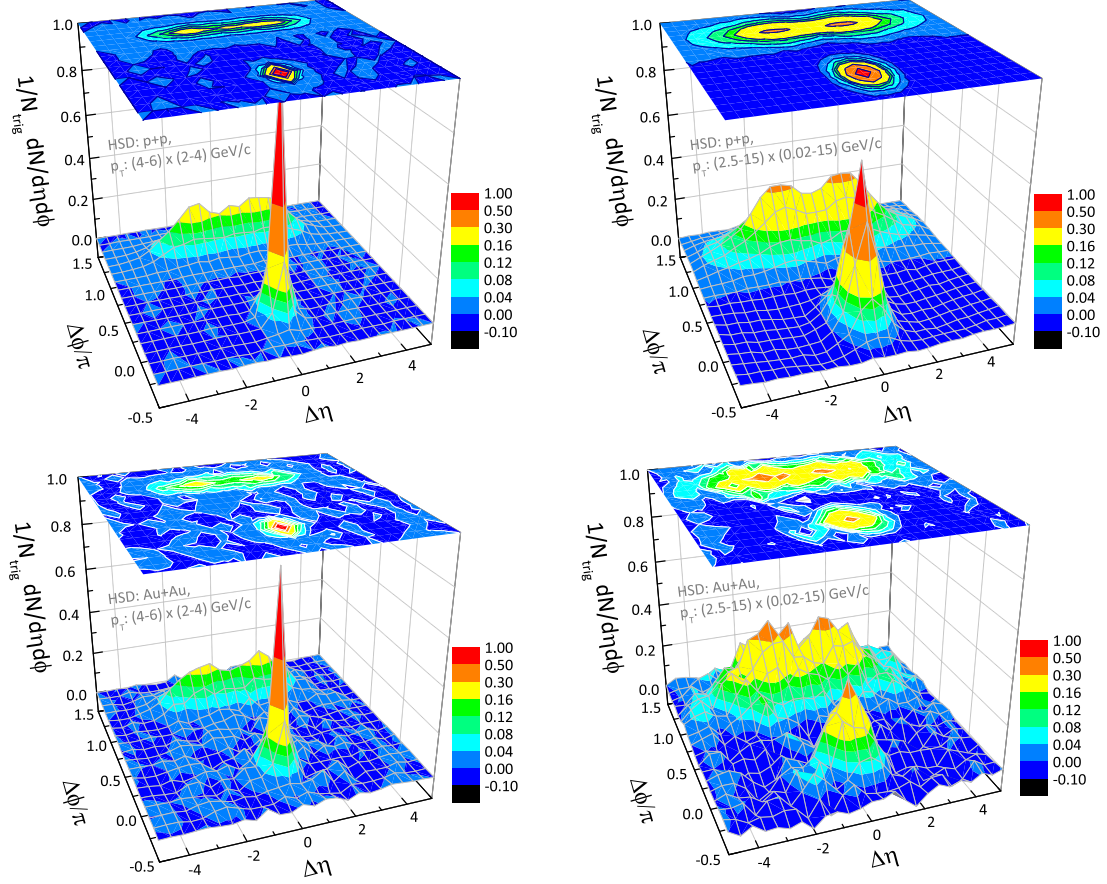


Fig. 5. The associated particle ($\Delta\eta$, $\Delta\phi$) distribution for p+p (*top panels*) and central Au+Au ($b=0$, *bottom panels*) collisions for the trigger hadron with $4 > p_T^{trig} > 6$ GeV/c (*left*) and $p_T^{trig} > 2.5$ GeV/c (*right*) within the HSD transport approach.

each trigger particle from another randomly chosen event.

Angular correlations of associated particles in p+p and central Au+Au collisions are shown in Figs. 3 and 4. There are two maxima: the ‘near-side’ and ‘away-side’ peaks at $\Delta\phi = 0$ and $\Delta\phi = \pi$, correspondingly. Fig. 3 provides a comparison to the data from the STAR Collaboration with the cuts for p_T^{trig} and p_T^{assoc} similar to those in the previous HSD calculations [23]. We find a good agreement between the earlier perturbative [23] and current non-perturbative HSD results. Thus, one may conclude that a medium modification in this kinematic region of p_T^{trig} and p_T^{assoc} is small in HSD. We mention that the HSD results reasonably reproduce the data for p+p collisions (within error bars). For Au+Au central collisions HSD shows clearly an insufficient suppression of the ‘away-side’ peak at $\Delta\phi/\pi = 1$. Note also that for the most central collisions the experimentally observed suppression of single-particle spectra at high- p_T can not fully be described by HSD: $R_{AA}^{HSD}(p_T) = 0.35 \div 0.4$ whereas $R_{AA}^{exp}(p_T) = 0.2 \div 0.25$ at $p_T > 4$ GeV/c. Our first conclusion is that the hadron-string medium is too transparent for high- p_T particles (as already pointed out in [23]).

Fig. 4 corresponds to the data of the PHENIX Collaboration with different cuts for

$p_T^{trig} = 2 \div 3$ GeV/c and $p_T^{assoc} = 0.4 \div 1$ GeV/c. This is the kinematic region where one expects a strong medium response to the jet energy loss. The experimental data show the presence of a ‘Mach-cone’ structure in azimuthal angle $\Delta\phi$ for the ‘away-side’ jet. This structure does not appear in the HSD simulations.

In Fig. 5 we present the HSD results for p+p and Au+Au collisions for the associated differential particle $(\Delta\eta, \Delta\phi)$ distribution. We use the same cuts as the STAR Collaboration, $4 < p_T^{trig} < 6$ GeV/c and $2 < p_T^{assoc} < 4$ GeV/c [20], and for the PHOBOS Collaboration, $p_T^{trig} > 2.5$ GeV and $p_T^{assoc} > 0.02$ GeV/c [21]. In the HSD transport calculations we obtain on average 0.5 and 5 trigger particles in an event for the STAR and PHOBOS set of cuts, correspondingly. The di-jet correlations obtained in the HSD transport simulations of Au+Au collisions (Fig. 5, *bottom* panels) do not show a ridge structure in pseudorapidity $\Delta\eta$ for the near-side jet as in the data [20,21].

Summary

The PHSD approach has been applied to nucleus-nucleus collisions from 20 to 160 A GeV in order to explore the space-time regions of ‘partonic matter’. We have found that even central collisions at the top SPS energy of ~ 160 A GeV show a large fraction of non-partonic matter. It is also found that though the partonic phase has only a very low impact on rapidity distributions of hadrons [3], it has a sizeable influence on the transverse-mass distribution of final kaons due to the repulsive partonic mean-fields and parton interactions. On the other hand, the most pronounced effect of the partonic phase is seen on the production of multi-strange antibaryons due to a slightly enhanced $s\bar{s}$ pair production in the partonic phase from massive time-like gluon decay and a more abundant formation of strange antibaryons in the hadronization process. We also mention that partonic production channels for dileptons appear to be visible in the $\mu^+\mu^-$ spectra from In+In collisions at 158 A·GeV in the intermediate invariant mass range [4].

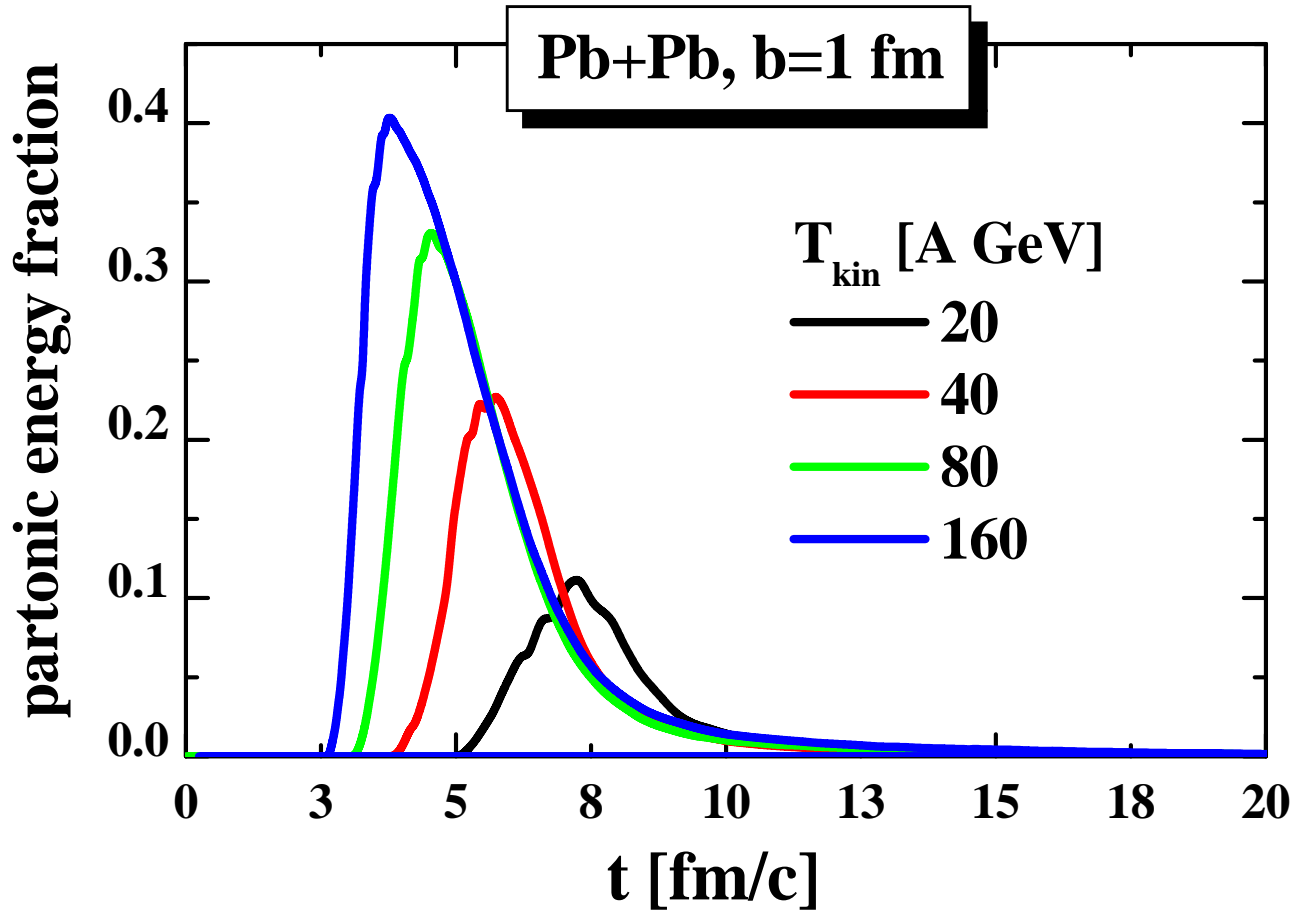
Additionally, we conclude that the HSD hadron-string medium does not show enough suppression for the nuclear modification factor $R_{AA}(p_T)$ at high p_T and for the away-side jet-associated particles. For the first time the medium response on the jet interactions has been taken into account in the present non-perturbative HSD calculations in extension to previous perturbative studies [6]. The non-perturbative calculations, however, do not reproduce the experimentally observed ‘Mach-cone’ structure in $\Delta\phi$ for the away-side jet and the long-range rapidity correlations (the ‘ridge’) for the near-side jet while supporting the results from the perturbative investigations. It is interesting to check in future whether the PHSD model – incorporating explicit partonic degrees of freedom and dynamical hadronization – will be able to improve an agreement with the data and reproduce the structures observed by the PHOBOS and STAR Collaborations.

Acknowledgments

Work supported in part by the ‘‘HIC for FAIR’’ framework of the ‘‘LOEWE’’ program.

References

- [1] W. Cassing and E. L. Bratkovskaya, Phys. Rev. C 78, 2008, P. 034919.
- [2] W. Cassing and S. Juchem, Nucl. Phys. A 665, 2000, P. 377; *ibid* A 672, 2000, P. 417.
- [3] W. Cassing and E. L. Bratkovskaya, Nucl. Phys. A 831, 2009, P. 215.
- [4] O. Linnyk, E. L. Bratkovskaya and W. Cassing, Nucl. Phys. A 830, 2009, P. 491C.
- [5] O. Linnyk, E. L. Bratkovskaya and W. Cassing, Int. J. Mod. Phys. E 17, 2008, P. 1367.
- [6] K. Gallmeister and W. Cassing, Nucl. Phys. A 748, 2005, P. 241.
- [7] L. P. Kadanoff and G. Baym, *Quantum Statistical Mechanics*, Benjamin, 1962.
- [8] S. Juchem *et al.*, Nucl. Phys. A 743, 2004, P. 92.
- [9] A. Peshier and W. Cassing, Phys. Rev. Lett. 94, 2005, P. 172301.
- [10] W. Cassing and E. L. Bratkovskaya, Phys. Rept. 308, 1999, P. 65; W. Ehehalt and W. Cassing, Nucl. Phys. A 602, 1996, P. 449.
- [11] W. Cassing, Nucl. Phys. A 791, 2007, P. 365; *ibid*. A 795, 2007, P. 70.
- [12] W. Cassing, E. L. Bratkovskaya and Y. Xing, Prog. Part. Nucl. Phys. 62, 2009, P. 359.
- [13] C. Alt *et al.*, NA49 Collaboration, Phys. Rev. C 66, 2002, P. 054902; Phys. Rev. C 77, 2008, P. 024903.
- [14] J. Geiss, W. Cassing and C. Greiner, Nucl. Phys. A 644, 1998, P. 107.
- [15] F. Antinori *et al.*, Phys. Lett. B 595, 2004, P. 68; J. Phys. G: Nucl. Phys. 32, 2006, P. 427.
- [16] T. Anticic *et al.* [NA49 Collaboration], Phys. Rev. C 80, 2009, P. 034906.
- [17] C. Alt *et al.*, NA49 Collaboration, Phys. Rev. C 78, 2008, P. 034918.
- [18] C. Adler *et al.* [STAR Collaboration], Phys. Rev. Lett. 90, 2003, P. 082302.
- [19] A. Adare *et al.* [PHENIX collaboration] Phys. Rev. C 78, 2008, P. 014901.
- [20] B. I. Abelev *et al.*, [STAR collaboration] Phys. Rev. C 80, 2009, P. 064912; M. van Leeuwen [STAR collaboration], Eur. Phys. J. C 61, 2009, P. 569.
- [21] B. Alver *et al.* [PHOBOS Collaboration], Phys. Rev. Lett. 104, 2010, P. 062301.
- [22] E. L. Bratkovskaya, S. Soff, H. Stöcker, M. van Leeuwen, and W. Cassing, Phys. Rev. Lett. 92, 2004, P. 032302;
- [23] W. Cassing, K. Gallmeister and C. Greiner, Nucl. Phys. A 735, 2004, P. 277; W. Cassing, K. Gallmeister and C. Greiner, J. Phys. G 30, 2004, P. S801;



Pb+Pb, 158 A GeV

